J|A|C|S
ARTICLES

Published on Web 06/08/2009

# Exploring the Reactivity of Ru-Based Metathesis Catalysts with a $\pi$-Acid Ligand Trans to the Ru−Ylidene Bond

Albert Poater, Francesco Ragone, Andrea Correa, and Luigi Cavallo*

*MoLNaC - Modeling Lab for Nanostructures and Catalysis, Dipartimento di Chimica, Università di Salerno, Via Ponte don Melillo, I-84084 Fisciano (SA), Italy*

Received March 31, 2009; E-mail: lcavallo@unisa.it

***Abstract:*** In this work we explore the reactivity induced by coordination of a CO molecule trans to the Ru−ylidene bond of a prototype Ru−olefin metathesis catalyst bearing the N-heterocyclic carbene (NHC) ligand SIMes. Static DFT calculations indicate that CO binding to the Ru center promotes a cascade of reactions with very low energy barriers that lead to the final crystallographically characterized product, in which the original methylidene group has attacked the proximal aromatic ring of the SIMes ligand leading to a cycloheptatriene through a Buchner ring expansion. Analysis of the relevant molecular orbitals, supported by *ab initio* molecular dynamics simulations, illuminate the key role of the $\pi$-acid CO coordinated trans to the Ru−methylidene bond to promote this reactivity. Based on this result, we investigated to which extent a large set of $\pi$-acid groups could promote this deactivating reaction. Results clearly indicate that almost any sufficiently $\pi$-acidic group that can approach the Ru center in the sterically crowded position trans to the Ru−methylidene bond can promote this deactivation route.

## Introduction

Ru-based catalysts for olefin metathesis have acquired a prominent role in modern organic synthesis[1] and are expanding from lab scale to industrial production. This step forward requires the design of very active and stable catalysts. Along this direction, replacement of a phosphine ligand with a N-heterocyclic carbene (NHC) ligand in Grubbs first generation catalysts[2] leads to NHC-based second generation catalysts that proved more active and in many cases even more stable.[3] The origin of the greater activity of NHC-based catalysts is now rather well understood, and despite being still incomplete,[4,5] this knowledge is currently used to approach the ambitious "rational design" of new catalysts. Unfortunately, stability remains an issue, and little is known about deactivation pathways, although work in this challenging area is increasing.[6,7] Broadly speaking, deactivation pathways are those chemical transformations of the (pre)catalyst or the active species that remove them from productive metathesis. In this sense, Diver, Keister, and co-workers[6,8,9] have clearly shown that addition of $\pi$ acids such as CO or isocyanides to a solution of typical second-generation catalysts can switch a metathesis catalyst into a cyclopropanation catalyst,[10] by activating the Ru−ylidene bond to a carbene-like reactivity. This promotes ylidene attack to the proximal N-bonded aromatic ring of the NHC ligand, which results in a Buchner type ring expansion reaction; see Scheme 1.

Although it is difficult to call the reaction of Scheme 1 a deactivation reaction, since CO is not normally added during

(1) Grubbs, R. H. *Handbook of Olefin Metathesis*; Wiley-VCH: Weinheim, Germany, 2003.
(2) Nguyen, S. T.; Grubbs, R. H.; Ziller, J. W. *J. Am. Chem. Soc.* **1993**, *115*, 9858–9859.
(3) (a) Scholl, M.; Ding, S.; Lee, C. W.; Grubbs, R. H. *Org. Lett.* **1999**, *1*, 953–956. (b) Huang, J.; Stevens, E. D.; Nolan, S. P.; Peterson, J. L. *J. Am. Chem. Soc.* **1999**, *121*, 2674–2678. (c) Weskamp, T.; Kohl, F. J.; Hieringer, W.; Gleich, D.; Herrmann, W. A. *Angew. Chem., Int. Ed.* **1999**, *38*, 2416–2419. (d) Bielawski, C. W.; Grubbs, R. H. *Angew. Chem., Int. Ed.* **2000**, *39*, 2903–2906.
(4) (a) Hoveyda, A. H.; Schrock, R. R. *Chem.—Eur. J.* **2001**, *7*, 945–950. (b) Schrock, R. R.; Hoveyda, A. H. *Angew. Chem., Int. Ed.* **2003**, *42*, 4592–4633. (c) Fürstner, A. *Angew. Chem., Int. Ed.* **2000**, *39*, 3012–3043. (d) Trnka, T. M.; Grubbs, R. H. *Acc. Chem. Res.* **2001**, *34*, 18–29.
(5) (a) Dias, E. L.; Nguyen, S. T.; Grubbs, R. H. *J. Am. Chem. Soc.* **1997**, *119*, 3887–3897. (b) Ulman, M.; Grubbs, R. H. *Organometallics* **1998**, *17*, 2484–2489. (c) Adlhart, C.; Hinderling, C.; Baumann, H.; Chen, P. *J. Am. Chem. Soc.* **2000**, *122*, 8204–8214. (d) Michrowska, A.; Bujok, R.; Harutyunyan, S.; Sashuk, V.; Dolgonos, G.; Grela, K. *J. Am. Chem. Soc.* **2004**, *126*, 9318–9325. (e) Getty, K.; Delgado-Jaime, M. U.; Kennepohl, P. *J. Am. Chem. Soc.* **2007**, *129*, 15774–15776. (f) van der Eide, E. F.; Romero, P. E.; Piers, W. E. *J. Am. Chem. Soc.* **2008**, *130*, 4485–4491. (g) Cavallo, L. *J. Am. Chem. Soc.* **2002**, *124*, 8965–8973. (h) Correa, A.; Cavallo, L. *J. Am. Chem. Soc.* **2006**, *128*, 13352–13353.
(6) Galan, B. R.; Gembicky, M.; Dominiak, P. M.; Keister, J. B.; Diver, S. T. *J. Am. Chem. Soc.* **2005**, *127*, 15702–15703.
(7) (a) Jazzar, R. F. R.; Macgregor, S. A.; Mahon, M. F.; Richards, S. P.; Whittlesey, M. K. *J. Am. Chem. Soc.* **2002**, *124*, 4944–4945. (b) Giunta, D.; Hölscher, M.; Lehmann, C. W.; Mynott, R.; Wirtz, C.; Leitner, W. *Adv. Synth. Catal.* **2003**, *345*, 1139–1145. (c) Abdur-Rashid, K.; Fedorkiw, T.; Lough, A. J.; Morris, R. H. *Organometallics* **2004**, *23*, 86–94. (d) Dorta, R.; Stevens, E. D.; Nolan, S. P. *J. Am. Chem. Soc.* **2004**, *126*, 5054–5055. (e) Scott, N. M.; Dorta, R.; Stevens, E. D.; Correa, A.; Cavallo, L.; Nolan, S. P. *J. Am. Chem. Soc.* **2005**, *127*, 3516–3526. (f) Hong, S. H.; Chlenov, A.; Day, M. W.; Grubbs, R. H. *Angew. Chem., Int. Ed.* **2007**, *46*, 5148–5151. (g) Berlin, J. M.; Campbell, K.; Ritter, T.; Funk, T. W.; Chlenov, A.; Grubbs, R. H. *Org. Lett.* **2007**, *9*, 1339–1342. (h) Hong, S. H.; Day, M. W.; Grubbs, R. H. *J. Am. Chem. Soc.* **2004**, *126*, 7414–7415. (i) Ulman, M.; Grubbs, R. H. *J. Org. Chem.* **1999**, *64*, 7202–7207. (j) Hong, S. H.; Wenzel, A. G.; Salguero, T. T.; Day, M. W.; Grubbs, R. H. *J. Am. Chem. Soc.* **2007**, *129*, 7961–7968. (k) Diver, S. T. *Coord. Chem. Rev.* **2007**, *251*, 671–701, references therein.
(8) After this manuscript was submitted for publication, an extended experimental work (ref 8) has been published by Diver, Keister, and co-workers.
(9) Galan, B. R.; Pitak, M.; Gembicky, M.; Keister, J. B.; Diver, S. T. *J. Am. Chem. Soc.* **2009**, *131*, 6822–6832.

 **10.1021/ja902552m CCC: $40.75** 

**Scheme 1**

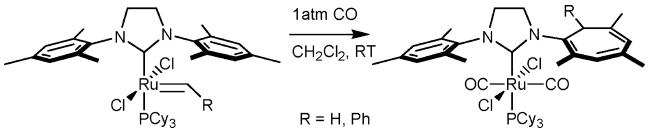


**Chart 1**

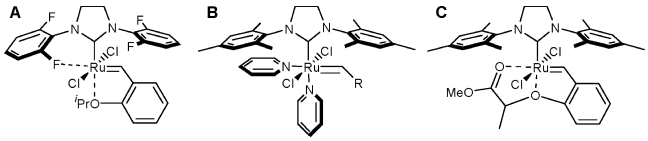


metathesis, understanding the chemistry behind this transformation is relevant for the following reasons. (1) $\pi$-Acids are inevitably present during metathesis, and any organometallic textbook presents educative comparisons between the $\sigma$-basic/$\pi$-acid properties of CO, olefins and phosphines. Clearly, olefins and phosphines are much weaker $\pi$-acids than CO, but a reduced acidity could still induce slow deactivation reactions as those shown in Scheme 1 for CO. (2) A clear understanding of the changes in the chemical behavior promoted by a $\sigma$-basic/$\pi$-acid ligand trans to the Ru−ylidene bond would expand our knowledge of the chemistry of Ru-based catalysts with possible consequences in the design of new ligands with tuned properties.

Indeed, the position trans to the Ru−ylidene bond has been scarcely considered during the years.[5c,11−13] For example, Grubbs and co-workers have suggested that one of the ortho-F atoms of the NHC **A** shown in Chart 1 could be engaged in an interaction with the Ru center that results in increased metathesis activity.[12] Furthermore, strategies for the synthesis of (pre)catalysts having labile ligands that could result in more stable and active catalysts, such as **B** and **C** of Chart 1, are explored.[13]

For these reasons we decided to investigate computationally the reactivity changes induced by a series of $\sigma$-basic/$\pi$-acid ligands coordinated trans to the Ru−methylidene bond of the systems shown in Chart 2. Such a systematic comparison should increase our understanding of the basic properties of the Ru−ylidene bond and of the reactivity changes that could in principle be induced by changes in the nature of the ligands connected to the Ru atom. Most of the calculations we present

**Chart 2**

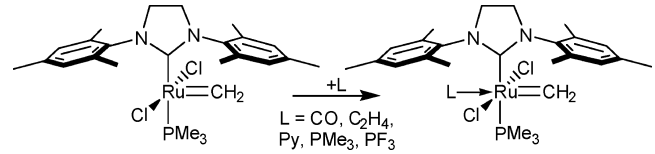


are based on a classical static density functional theory (DFT) approach, but we also performed a DFT based *ab initio* molecular dynamics (AIMD) simulation, which offers the invaluable opportunity to capture the time evolution of the reactive species.[14]

## Computational Details

All the DFT static calculations were performed at the GGA level with the Gaussian03 set of programs,[15] using the BP86 functional of Becke and Perdew.[16] The electronic configuration of the molecular systems was described with the standard split-valence basis set with a polarization function of Ahlrichs and co-workers for H, C, N, O, P, F, and Cl (SVP keyword in Gaussian).[17] For Ru we used the small-core, quasi-relativistic Stuttgart/Dresden effective core potential, with an associated (8s7p6d)/[6s5p3d] valence basis set contracted according to a (311111/22111/411) scheme (standard SDD keywords in gaussian03).[18] The geometry optimizations were performed without symmetry constraints, and the characterization of the located stationary points was performed by analytical frequency calculations. Solvent effects including contributions of nonelectrostatic terms have been estimated in single-point calculations on the gas phase optimized structures, based on the polarizable continuous solvation model PCM using $CH_2Cl_2$ as a solvent.[19] In conclusion, the energies reported correspond to the "Total free energy in solution: with all non electrostatic terms" value in the Gaussian output.

The AIMD simulations were performed using the Born−Oppenheimer scheme as implemented in the CP2K Quickstep code.[20,21] The electronic structure calculations were done at the DFT level using the Perdew−Burke−Ernzerhof exchange and correlation functional.[22] Within CP2K the Kohn−Sham molecular orbitals are described by a linear combination of Gaussian-type orbitals, whereas an auxiliary planewave basis set is employed to expand the electron density.[23] A double-$\zeta$ basis set with a polarization function,[20,24] in conjunction with the Goedecker−Teter−Hutter

(10) (a) Monnier, F.; Castillo, D.; Derien, S.; Toupet, L.; Dixneuf, P. H. *Angew. Chem., Int. Ed.* **2003**, *42*, 5474–5477. (b) Peppers, B. P.; Diver, S. T. *J. Am. Chem. Soc.* **2004**, *126*, 9524–9525. (c) Kitamura, T.; Sato, Y.; Mori, M. *Chem. Commun.* **2001**, 1258–1259. (d) Nishiyama, H.; Itoh, Y.; Matsumoto, H.; Park, S.-B.; Itoh, K. *J. Am. Chem. Soc.* **1994**, *116*, 2223–2224. (e) Anciaux, A. J.; Demonceau, A.; Noels, A. F.; Hubert, A. J.; Warin, R.; Teyssie, P. *J. Org. Chem.* **1981**, *46*, 873–876. (f) Basato, M.; Tubaro, C.; Biffis, A.; Bonato, M.; Buscemi, G.; Lighezzolo, F.; Lunardi, P.; Vianini, C.; Benetollo, F.; Del Zotto, A. *Chem.—Eur. J.* **2009**, *15*, 1516–1526.
(11) Webster, C. E. *J. Am. Chem. Soc.* **2007**, *129*, 7490–7491.
(12) Ritter, T.; Day, M. W.; Grubbs, R. H. *J. Am. Chem. Soc.* **2006**, *128*, 11768–11769.
(13) (a) Sanford, M. S.; Love, J. A.; Grubbs, R. H. *Organometallics* **2001**, *20*, 5314–5318. (b) Bieniek, M.; Bujok, R.; Cabaj, M.; Lugan, N.; Lavigne, G.; Arlt, D.; Grela, K. *J. Am. Chem. Soc.* **2006**, *128*, 13652–13653.
(14) (a) Car, R.; Parrinello, M. *Phys. Rev. Lett.* **1985**, *55*, 2471–2474. (b) Kuhne, T. D.; Krack, M.; Mohamed, F. R.; Parrinello, M. *Phys. Rev. Lett.* **2007**, *98*, 066401–4. (c) Marx, D.; Hutter, J. In *Ab initio molecular dynamics: Theory and Implementation, Modern Methods and Algorithms of Quantum Chemistry*; Grotendorst, J., Ed.; John von Neumann Institute for Computing: Jülich, Germany, 2000; NIC Series, Vol. 1, pp 301−449.
(15) Frisch, M. J. et al. *Gaussian03*, revision E.01; Gaussian, Inc.: Wallingford, CT, 2004.
(16) (a) Becke, A. *Phys. Rev. A* **1988**, *38*, 3098–3100. (b) Perdew, J. P. *Phys. Rev. B* **1986**, *33*, 8822–8824. (c) Perdew, J. P. *Phys. Rev. B* **1986**, *34*, 7406–7406.
(17) Schaefer, A.; Horn, H.; Ahlrichs, R. *J. Chem. Phys.* **1992**, *97*, 2571–2577.
(18) (a) Haeusermann, U.; Dolg, M.; Stoll, H.; Preuss, H. *Mol. Phys.* **1993**, *78*, 1211–1224. (b) Kuechle, W.; Dolg, M.; Stoll, H.; Preuss, H. *J. Chem. Phys.* **1994**, *100*, 7535–7542. (c) Leininger, T.; Nicklass, A.; Stoll, H.; Dolg, M.; Schwerdtfeger, P. *J. Chem. Phys.* **1996**, *105*, 1052–1059.
(19) (a) Barone, V.; Cossi, M. *J. Phys. Chem. A* **1998**, *102*, 1995–2001. (b) Tomasi, J.; Persico, M. *Chem. Rev.* **1994**, *94*, 2027–2094.
(20) Kohlmeyer, A.; Mundy, C. J.; Mohamed, F.; Schiffmann, F.; Tabacchi, G.; Forbert, H.; Kuo, W.; Hutter, J.; Krack, M.; Iannuzzi, M.; McGrath, M.; Guidon, M.; Kuehne, T. D.; Laino, T.; VandeVondele, J.; Weber, V. CP2K, http://cp2k.berlios.de, 2004.
(21) VandeVondele, J.; Krack, M.; Mohamed, F.; Parrinello, M.; Chassaing, T.; Hutter, J. *Comput. Phys. Commun.* **2005**, *167*, 103–128.
(22) Perdew, J. P.; Burke, K.; Ernzerhof, M. *Phys. Rev. Lett.* **1996**, *77*, 3865–3868.
(23) Lippert, G.; Hutter, J.; Parrinello, M. *Mol. Phys.* **1997**, *92*, 477–487.
(24) Krack, M.; Parrinello M. In *High Performance Computing in Chemistry*; Grotendorst, J., Ed.; Research Centre Jülich: Jülich, Germany, 2004; NIC series, Vol. *25*, pp 29−51.

pseudopotentials,[25] was used for all the atoms (standard DZVP-GTH in CP2K). The auxiliary planewave basis set was defined by a cubic box of 20 × 20 × 20 Å$^3$ and by an energy cutoff of 300 Ry. The equations of motion were integrated using a time step of 0.5 fs. A harmonic constraint centered at 3.0 Å with a force constant of 15 kcal/mol was applied on the Ru−CO distance, and the system was equilibrated for 0.5 ps by imposing that the temperature was held within 300 K ± 10 K by rescaling atomic velocities. After equilibration the system was sampled in the NVE ensamble for 5 ps. After the first picosecond, the constraint on the Ru−CO distance was removed and the system was allowed to evolve freely.

The electrophilicity of the complexes was evaluated as the Parr electrophilicity index shown in eq 1:[26]

$$\omega = \frac{\mu^2}{2\eta} \tag{1}$$

where $\mu$ and $\eta$ are the chemical potential and the molecular hardness, respectively. In the framework of DFT,[27] $\mu$ and $\eta$ for a N-electron system with total electronic energy $E$ and subject to an external potential are defined as the first and second derivatives of the energy with respect to N at a fixed external potential.[28] In numerical applications, $\mu$ and $\eta$ are approximated with the finite difference formulas of eq 2, which are based on Koopmans' theorem,[29]

$$\mu \cong \frac{1}{2}(\varepsilon_L + \varepsilon_H) \text{ and } \eta \cong \frac{1}{2}(\varepsilon_L - \varepsilon_H) \tag{2}$$

where $\epsilon_H$ and $\epsilon_L$ are the energies of the highest occupied molecular orbital (HOMO) and the lowest unoccupied molecular orbital (LUMO), respectively.

The strength of the Ru−ylidene bond was evaluated with the Mayer Bond Order (MBO),[30] which is a valuable tool in the analysis of the bonding in main group compounds and has been also used to characterize transition metal systems.[31,32]

Finally, in some cases we discuss the change in the local aromaticity of a given ring. As a structure-based measure, we have used the Kruszewski and Krygowski harmonic oscillator model of aromaticity (HOMA) index; see eq 3:[33]

$$\text{HOMA} = 1 - \frac{\alpha}{n}\sum_{i-1}^{n}(R_{opt} - R_i)^2 \tag{3}$$

where $n$ is the number of bonds considered, $R_i$ are the bond lengths, and $\alpha$ is an empirical constant (for C−C bonds $\alpha = 257.7$) fixed to give HOMA = 0 for a model nonaromatic system and HOMA = 1 for a system with all the bonds equal to their optimal value $R_{opt}$, which is 1.388 Å for C−C bonds (i.e., the bond length in fully aromatic systems).

## Results

We begin discussing the effect of a CO molecule coordinated trans to the Ru=$CH_2$ bond, since clean experimental data are available for this system. Starting from precatalyst **1a**, the first step corresponds to coordination of a CO molecule to the vacant coordination position trans to the Ru=$CH_2$ bond. The binding energy of the CO molecule to the Ru atom in **2a** is 22.5 kcal/mol. Coordination of the CO molecule has a strong effect on the Ru=$CH_2$ bond, which elongates from 1.81 Å in **1a** to 1.92 Å in **2a**, and pushes the phosphine almost perfectly trans to the NHC ligand, with a small elongation (less than 0.04 Å) of the Ru−NHC and Ru−P bonds. CO coordination also results in the remarkable reduction of the NHC−Ru=$CH_2$ angle from 103.9° in **1a** to 93.9° in **2a**, thus increasing the proximity of the reactive methylidene group with the proximal aromatic ring of the SIMes ligand (the $C_{methylidene}$−$C_{ipso}$ distance reduces from 3.56 to 2.62 Å).

At this point, the cyclopropanation reaction between the methylidene group and one of the $C_{ipso}$−$C_{ortho}$ bonds of the nearby mesityl ring occurs in two steps. The former corresponds to attack of the methylidene group to the $C_{ipso}$ atom, which requires overcoming the negligible barrier of 0.7 kcal/mol and leads to **3a**, which still presents a Ru−$CH_2$ bond and is only 3.7 kcal/mol more stable than **2a** (Figure 1). The second step of the cyclopropanation reaction requires the complete rupture of the Ru−$CH_2$ bond with the concerted formation of a cyclopropane ring by attack of the $C_{methylidene}$ atom to one of the $C_{ortho}$ atoms of the mesityl ring. This step requires overcoming a barrier of 0.3 kcal/mol only, after which the system collapses into the quite stable intermediate **4a**, 15.0 kcal/mol below the CO coordinates species **2a**. Intermediate **4a** presents a vacant coordination position trans to the CO. Analysis of the Mayer bond orders indicated that transition state **[2a-3a]** is highly concerted, since the bond orders of the breaking $\pi$ Ru−$C_{methylidene}$ bond and of the forming $C_{methylidene}$−$C_{ipso}$ bond in transition state **[2a-3a]** are halfway (0.99 and 0.53, respectively) between the values in **2a** (1.48 and 0.14) and **3a** (0.60 and 0.91). Conversely, **[3a-4a]** can be classified as an early transition state, since the bond orders of the breaking $\sigma$ Ru−$C_{methylidene}$ bond and of the forming $C_{methylidene}$−$C_{ortho}$ bond in **[3a-4a]** (0.56 and 0.23, respectively) are clearly closer to the values in **2a** (0.60 and 0.15) than in **3a** (0.17, 0.87).

Overall, considering the rather small energy barriers associated with the **2a** → **3a** and **3a** → **4a** steps, it is reasonable to hypothesize that kinetically formation of the cyclopropane intermediate **4a**, after CO coordination, occurs in a single step from **2a** down to **4a**.

(25) (a) Goedecker, S.; Teter, M.; Hutter, J. *Phys. Rev. B* **1996**, *54*, 1703–1710. (b) Krack, M. *Theor. Chem. Acc.* **2005**, *114*, 145–152.
(26) Parr, R. G.; von Szentpaly, L.; Liu, S. *J. Am. Chem. Soc.* **1999**, *121*, 1922–1924.
(27) Geerlings, P.; De Proft, F.; Langenaeker, W. *Chem. Rev.* **2003**, *103*, 1793–1873.
(28) (a) Parr, R. G.; Yang, W. *Density Functional Theory of Atoms and Molecules*; Oxford University Press: New York, 1989. (b) Parr, R. G.; Donnelly, R. A.; Levy, M.; Palke, W. E. *J. Chem. Phys.* **1978**, *68*, 3801–3807. (c) Parr, R. G.; Pearson, R. G. *J. Am. Chem. Soc.* **1983**, *105*, 7512–7516.
(29) Koopmans, T. *Physica* **1934**, *1*, 104–113.
(30) (a) Mayer, I. *Chem. Phys. Lett.* **1983**, *97*, 270. (b) Mayer, I. *Int. J. Quantum Chem.* **1984**, *26*, 151–154.
(31) (a) Bridgeman, A. J.; Harris, N.; Young, N. A. *Chem. Commun.* **2000**, 1241–1242. (b) Bridgeman, A. J.; Nielsen, N. A. *Inorg. Chim. Acta* **2000**, *303*, 107–115. (c) Bridgeman, A. J.; Rothery, J. *J. Chem. Soc., Dalton Trans.* **1999**, 4077–4082. (d) Bridgeman, A. J.; Rothery, J. *Inorg. Chim. Acta* **1999**, *288*, 17–28. (e) Bridgeman, A. J. *Polyhedron* **1998**, *17*, 2279–2288. (f) Bridgeman, A. J. *J. Chem. Soc., Dalton Trans.* **1997**, 2887–2893. (g) Bridgeman, A. J. *J. Chem. Soc., Dalton Trans.* **1997**, 1323–1329.
(32) (a) Bridgeman, A. J.; Rothery, J. *J. Chem. Soc., Dalton Trans.* **2000**, 211–218. (b) Bridgeman, A. J. *J. Chem. Soc., Dalton Trans.* **1996**, 2601–2607. (c) Bridgeman, A. J. *J. Chem. Soc., Dalton Trans.* **1997**, 4765–4771. (d) Bridgeman, A. J.; Bridgeman, C. H. *Chem. Phys. Lett.* **1997**, *272*, 173–177. (e) Bridgeman, A. J.; Cavigliasso, G.; Ireland, L. R.; Rothery, J. *J. Chem. Soc., Dalton Trans.* **2001**, 2095–2108. (f) Poater, A.; Duran, M.; Jaque, P.; Toro-Labbé, A.; Solà, M. *J. Phys. Chem. B* **2006**, *110*, 6526–6536. (g) Poater, A.; Moradell, S.; Pinilla, E.; Poater, J.; Solà, M.; Martínez, M. A.; Llobet, A. *Dalton Trans.* **2006**, 1188–1196.
(33) (a) Kruszewski, J.; Krygowski, T. M. *Tetrahedron Lett.* **1972**, 3839–3842. (b) Krygowski, T. M. *J. Chem. Inf. Comput. Sci.* **1993**, *33*, 70–78.

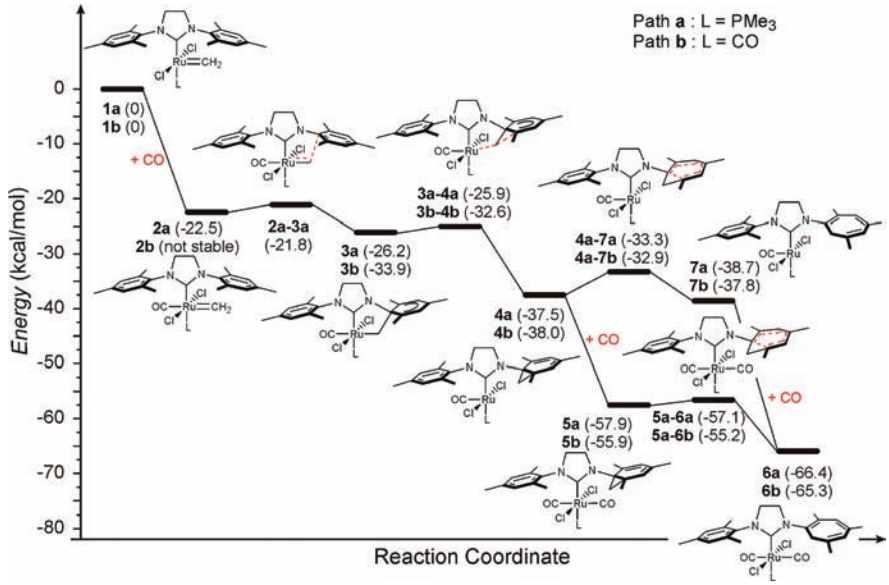


***Figure 1.*** Energy diagram of the complete **1** to **6** deactivation pathway. In parentheses is the energy of the various species, in kcal/mol, relative to the (pre)catalyst **1a**.

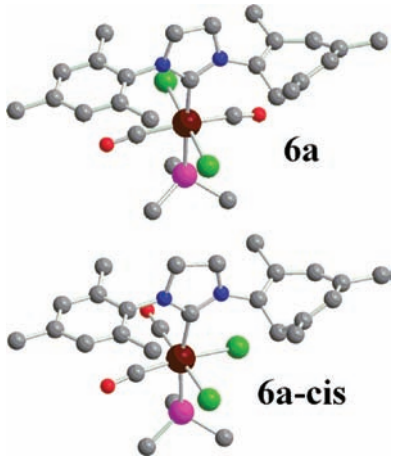


***Figure 2.*** Kinetic trans (**6a**) and thermodynamic cis (**6a-cis**) isomers of the decomposition product.

Coordination of a second CO molecule to **4a** is a barrierless process and leads to intermediate **5a**. The binding energy of the second CO molecule, 20.4 kcal/mol, is comparable to the binding energy of the first CO in **2a**, 22.5 kcal/mol. At this point, the only step needed to form the experimentally observed product is the opening of the $C_{ipso}-C_{ortho}$ bond of the tensioned cyclopropane ring of **5a**, which leads to product **6a**, overcoming yet another small energy barrier, 0.8 kcal/mol in this case. We also examined the cyclopropane opening in the absence of a second CO molecule coordinated to the Ru atom. In this case the somewhat larger barrier of 4.2 kcal/mol must be passed, after which the system collapses into intermediate **7a**. After the cyclopropane ring is opened, coordination of a second CO molecule leads to the final product **6a**. Considering the small energy barrier for the **4a** → **7a** step, it is possible that coordination of the second CO molecule occurs after the ring expansion step.

Product **6a**, shown in Figure 2, is the only species for which X-ray data are available. Geometrical analysis indicates that the computed structure is in excellent agreement with the crystallographic structure, with a rmsd of 0.032 Å for distances and of 0.8° for angles.[34] This also indicates that the sterically demanding $PCy_3$ phosphine can be safely replaced with the less bulkier $PMe_3$ phosphine to shed light on this kind of reactions.

As suggested by Diver and co-workers, we explored alternative geometries for **6a**, since complexes of generic formula $Ru(CO)_2X_2L_2$ (where X is a halide or pseudohalide and L is a neutral donor ligand) usually present a stable $Ru(cis\text{-}CO)_2(cis\text{-}X)_2(trans\text{-}L)_2$ geometry.[35] Four different isomers with a *cis*-CO and *cis*-Cl geometry are possible, since the NHC ligand is $C_1$ symmetric after formation of the seven-membered cycle. All of them are roughly 10 kcal/mol lower in energy than the *trans* isomer **6a**, with the most stable isomer, **6a-cis** shown in Figure 2, 10.4 kcal/mol more stable that **6a**. These results support the hypothesis of Diver and co-workers that **6a** corresponds to the kinetic product of the reaction[6] and that isomerization between the trans and cis isomers is not an easy process.

The reaction pathway when the phosphine of precatalyst **1a** is substituted by a CO molecule leading to **1b** is also shown in Figure 1. Energetically, substitution of $PMe_3$ with CO is almost thermoneutral, since the CO binding energy is only 1.3 kcal/mol larger than that of $PMe_3$, although this substitution probably requires dissociation of $PMe_3$ from **1a**, which costs 27.8 kcal/mol. Coordination of a second CO molecule trans to the Ru−methylidene bond of **1b** does not lead to an intermediate analogous to **2a**. Instead, all the geometry optimizations we tried inevitably collapsed into species **3b**, in which the $C_{methylidene}-C_{ipso}$ bond is already formed. Beside this difference,

(34) Standard deviations for distances and angles:

$$S_{n-1} = \sqrt{\frac{\sum_{i=1}^{N}(\mathrm{CV} - \mathrm{EV})^2}{N-1}}$$

where CV means calculated value, EV experimental value (X-ray data), and $N$ is the number of distances or angles taken into account (distances and angles used are given in Table S2 of the Supporting Information).

(35) (a) Krassowski, D. W.; Nelson, J. H.; Broer, K. R.; Hauenstein, D.; Jacobson, R. A. *Inorg. Chem.* **1988**, *27*, 4294–4307. (b) Barnard, C. F. J.; Daniels, J. A.; Jeffrey, J.; Mawby, R. J. *J. Chem. Soc., Dalton Trans.* **1976**, 953–961.

*Scheme 2*

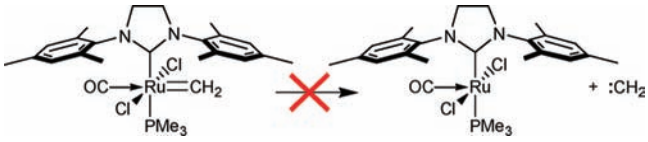

the energy profile with a CO molecule trans to the NHC ligand (path **b** in Figure 1) is rather similar to that with a $PMe_3$ molecule trans to the NHC ligand (path **a** in Figure 1). Our inability to locate intermediate **2b** indicates that the CO molecule trans to the NHC ligand contributes to weaken the Ru−ylidene bond, activating it toward the proximal mesityl ring. Considering the relative size of the $PMe_3$ and CO ligands in **1a** and **1b**, it is clear that the effect of the second CO ligand is almost entirely electronic in nature. The activating effect of the CO coordinated trans to the NHC ligand is also evidenced by the increase of the Parr electrophilicity index,[19,36] which increases from 112.1 in **1a** to 174.7 kcal/mol in **1b**. However it is coordination of a CO molecule trans to the Ru−ylidene bond the key factor facilitating attack of the methylidene group to the proximal mesityl ring. This point is reinforced by observing that the aromaticity of this mesityl ring is comparable in **1a** and **1b**, as indicated by very similar HOMA indexes, 0.834 and 0.838, respectively.

## Discussion

As already indicated, methylidene attack to one of the aromatic rings of the SIMes ligand with formation of a cycloheptatriene type ring corresponds to a classical Buchner ring expansion reaction. To understand the chemistry behind this reaction, we first tested the possibility that CO coordination could induce the release of a free carbene, as shown in Scheme 2. However, the reaction of Scheme 2 is endoergonic by 40.7 kcal/mol, which rules out this possibility and is in agreement with the experimental nondetection of regioisomers due to remote cyclopropanation of aromatic $\pi$-bonds, as could occur in the presence of free carbene.[6]

To rationalize the activation role of the CO, Diver and co-workers suggested that CO binding may weaken $\pi$-back-bonding between the Ru atom and the ylidene ligand, making the latter more electrophilic and disengaging it from the metal center. To verify this hypothesis we performed a comparative molecular orbital (MO) analysis of complexes **1a** and **2a**. Results can be summarized considering the MO diagram reported in Scheme 3.

In the precatalyst **1a** the classical Fischer carbene bonding scheme is established.[37] Electron density is donated from filled d orbitals on the Ru to the empty $\pi$ orbital of the methylidene. Differently, in the presence of the strong $\pi$-acid CO molecule, electron density from the Ru is more strongly donated to $\pi$-acid MOs of the CO. As suggested by Diver, this depletes electron density from the $\pi$ orbital of the methylidene, which is able to accept from the properly oriented $\pi$ orbital of the $C_{ipso}$ atom of the proximal ring, resulting in a very low barrier for formation of the $C_{methylidene}-C_{ipso}$ bond. Natural bond order (NBO) analysis

*Scheme 3*

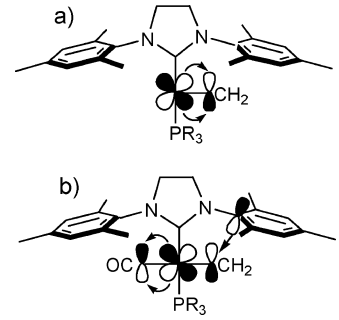

of the $Ru-C_{methylidene}$ bond supports this view. In fact, in species **1a** the MO corresponding to the $\pi$ $Ru-C_{methylidene}$ bond is 62% Ru and 38% $C_{methylidene}$. After CO coordination, which is in **1b**, this MO becomes 75% Ru and 25% $C_{methylidene}$. Interestingly, a similar analysis of the $\sigma$ $Ru-C_{methylidene}$ bond indicates that in **1a** this bond is 47% Ru and 53% $C_{methylidene}$, while in **1b** (due to the strong trans effect of the CO) this MO becomes 35% Ru and 65% $C_{methylidene}$. In short, after CO coordination the methylidene has greater "free-carbene" character. Consequently, in the **3a** → **4a** step the $C_{methylidene}$ atom is able to attack with a low energy barrier one of the $C_{ortho}$ atoms of the N-bonded ring that, incidentally, is also activated by the loss of aromaticity after formation of the $C_{methylidene}-C_{ipso}$ bond.

Other evidence of the incipient interaction between the $\pi$-orbitals of the methylidene C atom and of the $C_{ipso}$ atom of the proximal mesityl ring is the decrease of the HOMA index of this mesityl ring that drops from 0.834 in **1a** to 0.787 in **2a** and the decrease of the Mayer Bond Order of the $Ru=CH_2$ bond that drops from 2.015 in **1a** to 1.479 in **2a**.

The chemical consequence of this interaction is in the higher reactivity of **2a** with respect to **1a**, as indicated by the increase of the Parr electrophilicity index[19,36] from 112.1 kcal/mol in **1a** to 212.1 kcal/mol in **2a**. This change in electrophilicity is a consequence of the increased stability of the LUMO, which results in a smaller HOMO−LUMO gap and thus in decreased chemical hardness (21.3 and 16.3 kcal/mol for species **1a** and **2a**, respectively).

To characterize dynamically this reaction we performed an *ab initio* molecular dynamics simulation starting from precatalyst **1a** with a CO molecule constrained to be at 3.0 Å from the Ru center. The most relevant structural fluctuations of the system are reported in Figure 3

During the first picosecond, with the CO molecule constrained at 3.0 Å from the Ru center, only small

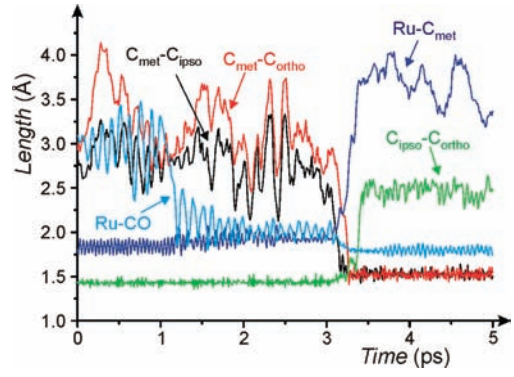


***Figure 3.*** Time evolution of the most relevant distances during the AIMD simulation. $C_{met}$ stands for $C_{methylidene}$.

(36) (a) Costas, M.; Ribas, X.; Poater, A.; López-Valbuena, J. M.; Xifra, R.; Company, A.; Duran, M.; Solà, M.; Llobet, A.; Corbella, M.; Usón, M. A.; Mahia, J.; Solans, X.; Shan, X. P.; Benet-Buchholz, J. *Inorg. Chem.* **2006**, *45*, 3569–3581. (b) Jaque, P.; Toro-Labbé, A. *J. Chem. Phys.* **2002**, *117*, 3208–3218.

(37) Frenking, G.; Solà, M.; Vyboishchikov, S. F. *J. Organomet. Chem.* **2005**, *690*, 6178–6204.

***Scheme 4***

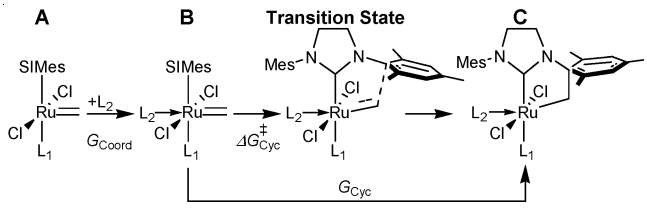


oscillations in the Ru−methylidene and $C_{ipso}-C_{ortho}$ bond distances are observed. Larger oscillations are visible for the $C_{methylidene}-C_{ipso}$ distance, but the minimum value never is below 2.5 Å, due to the repulsive interaction between the filled $\pi$ MO on the methylidene C atom and the aromatic $\pi$ MOs of the mesityl ring, which is consistent with the MO picture of Scheme 3a. During the first picosecond the Ru−CO distance oscillates broadly around 3.0 Å, and CO coordination to the Ru center is forbidden by the constraint. Indeed, after release of this constraint, which is after 1 ps, the CO coordinates rapidly to the Ru center with a damped oscillating behavior centered around a value of ∼2 Å. Interestingly, as the Ru−CO distance stabilizes, that is at ∼1.5−2.0 ps, larger oscillations start in the $C_{methylidene}-C_{ipso}$ distance, with peaks at the low values of 2 Å at ∼2.0−2.5 ps. Such a short distance is possible because of the transfer of the Ru electron density from the $\pi$ MO on the methylidene C atom to the $\pi$-acid MO of the CO, consistent with the MO picture of Scheme 3b. Accidentally, at ∼3.2 ps one of these oscillations overcomes the repulsive forces between the $C_{methylidene}$ and $C_{ipso}$ atoms (i.e., the system overcomes the transition state **2a-3a** of Figure 1), and the system collapses rapidly into structure **3a**, with clean formation of the $C_{methylidene}-C_{ipso}$ bond. Almost immediately, complete rupture of the Ru−methylidene bond of **3a** is observed, with simultaneous formation of intermediate **4a** that, under our simulation conditions, is stable for a very short time between 3.2 and 3.4 ps. In fact, the Buchner expansion step occurs rapidly and the system reaches the final product **7a**, with rupture of the $C_{ipso}-C_{ortho}$ bond, at ∼3.6 ps. The heptatriene product **7a** is rather stable in the last 1.4 ps of the simulation, suggesting that dynamically **7a** is favored over the almost isoenergetic species **4a**, probably due to a larger conformational freedom in **7a**. This series of events suggests that cyclopropane rupture occurs prior to coordination of the second CO molecule.

At this point we wondered to which extent this reaction could occur without a ligand trans to the Ru−ylidene bond or, alternatively, in the presence of a $\pi$-acid weaker than CO, such as olefins, phosphines, or pyridine, which are typically present during metathesis or, finally, with methyl isocyanide, a ligand used experimentally by Diver, Keister, and co-workers.[6] To this end we investigated the first step of the cyclopropanation reaction (see Scheme 4) in the absence of any ligand, in the presence of an ethene molecule (to model the C=C double bond of any substrate), and in the presence of a pyridine, a $PMe_3$, or a $PF_3$ molecule (to model typical labile ligands). $PF_3$ is chosen as an example of a rather $\pi$-acid phosphine. On the other hand, we also varied the nature of the ligand trans to the NHC ligand.

The results for the various ligands are shown in Table 1. First of all, with no $L_2$ ligand trans to the Ru−methylidene bond, i.e., in system **1a**, entry 1 in Table 1, the metallacycle structure **C** of Scheme 4 is not stable. All our attempts to locate a metallacycle structure similar to **3a** in the absence of an $L_2$ ligand failed, and the geometry optimization collapsed into the starting species **1a**. In the case of $L_2$ = CO, entry 2 in Table 1, as already discussed in the Results section, the $L_2$ coordinated species **2a** and the metallacycle species **3a** (corresponding to **B** and **C** in Scheme 4) are stable, though the metallacycle **3a** is favored relative to **2a** by 3.7 kcal/mol. In the presence of the weak $\pi$-acid C=C double bond of an ethene molecule as well as in the presence of a pyridine molecule trans to the Ru−methylidene bond, entries 3 and 4 in Table 1, the metallacycle **C** is not stable. Indeed, ethene coordination to **1a** is even disfavored by 1.8 kcal/mol, probably due to steric crowding around the metal that prevents the ethene molecule to assume a proper orientation (i.e., parallel to the NHC−Ru−P axis) to interact effectively with filled d orbitals of the metal.[38] On the other hand, pyridine coordination to **1a** is favored by 6.1 kcal/mol, thanks to its $\sigma$-donicity and flat geometry, but its lacks the required $\pi$-acid property to destabilize the Ru−methylidene bond and thus pyridine is unable to stabilize the metallacycle.

***Table 1.*** Energetics, in kcal/mol, of the First Step of the Cyclopropanation Reaction Shown in Scheme 4 and Electrophilicity, $\omega$, of the Species with the $L_2$ Ligand Coordinated to the Ru Atom

| | $L_1$ | $L_2$ | $\omega$ | $G_{Coord}$ | $\Delta G^{\ddagger}_{Cyc}$ | $G_{Cyc}$ |
|---|---|---|---|---|---|---|
| 1 | $PMe_3$ | none | − | − | − | not stable |
| 2 | $PMe_3$ | CO | 212.1 | −22.5 | 0.7 | −3.7 |
| 3 | $PMe_3$ | ethene | 139.8 | 1.8 | − | not stable |
| 4 | $PMe_3$ | pyridine | 143.2 | −6.1 | − | not stable |
| 5 | $PMe_3$ | $PMe_3$ | 138.5 | 3.6 | 1.9 | −0.7 |
| 6 | $PMe_3$ | $PF_3$ | 216.1 | −12.0 | 0.2 | −3.4 |
| 7 | $PMe_3$ | $NH_3$ | 112.9 | −13.2 | − | not stable |
| 8 | $PMe_3$ | $PH_3$ | 145.7 | −7.7 | 5.0 | 4.6 |
| 9 | $PMe_3$ | MeNC | 152.6 | −17.7 | 3.8 | 2.7 |
| 10 | pyridine | none | − | − | − | not stable |
| 11 | pyridine | CO | 228.3 | −19.4 | −0.5 | −7.0 |
| 12 | pyridine | pyridine | 149.7 | −6.9 | − | not stable |
| 13 | $PF_3$ | $PF_3$ | − | not stable | − | −26.2[a] |
| 14 | CO | CO | − | not stable | − | −33.9[a] |

[a] $G_{Cyc}$ calculated relative to the species with $L_2$ dissociated from Ru.

This conceptual scheme is somewhat confirmed by the behavior of the systems with $L_2$ = $PMe_3$ and $PF_3$, entries 5 and 6 in Table 1, the latter a prototype of very electron-poor phosphites, which also have moderately strong $\pi$-stabilization properties. In these cases both species **B** and **C** of Scheme 4 are stable, and the metallacycle structure **C** is slightly more stable than the coordinated species **B** in the case of the more acidic $PF_3$ phosphine (by 3.7 kcal/mol) than in the case of the less acidic $PMe_3$ phospine (by 0.7 kcal/mol). At this point the behavior with $L_2$ = $NH_3$, entry 7 in Table 1, is rather obvious. In fact, differently from phosphines, amines do not show $\pi$-acid properties, which explains why $NH_3$ is unable to stabilize the metallacycle **C**. Remarkably, a small $PH_3$ ligand coordinates favorably trans to the Ru−methylidene bond, entry 8 in Table 1, which clearly indicates that the mesityl rings of the SIMes ligand shields remarkably this position, which would be otherwise reactive.

Replacing the $L_1$ $PMe_3$ ligand with a pyridine has a minor effect on the behavior of the system (compare entries 10−12 in Table 1 with entries 1, 2, and 4) while replacing both $L_1$ and $L_2$ with stronger $\pi$-acids such as CO and $PF_3$ (entries 13 and 14 in Table 1) results in a reduction of the barrier separating the coordinated

(38) This point is also discussed in a paper (ref 8) published after this manuscript was submitted for publication.

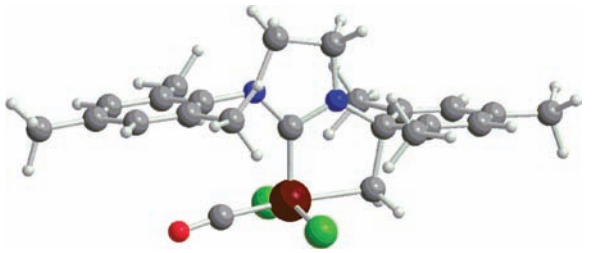

***Figure 4.*** Structure of the optimized geometry after removal of the $PMe_3$ ligand from **2a**.

***Chart 3***

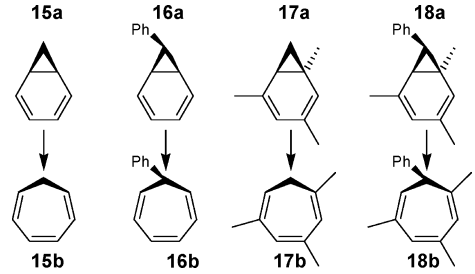


species **A** from the metallacycle species **C** that, remarkably, becomes the only stable structure. The electrophilicity of the species with the $L_2$ ligand coordinated to the Ru atom indicates that the higher the electrophilicity, the higher the reactivity of the methylidene group toward the $C_{ipso}$. This is reasonable, considering that the LUMO of the species with the $L_2$ ligand coordinated to the Ru atom mostly corresponds to the $\pi$ MO on the methylidene group.

Interestingly, in all the cases where both structures **A** and **C** are stable, the energy barrier for the **A** → **C** conversion is rather small. This indicates that an $L_2$ $\pi$-acid ligand trans to the Ru−ylidene bond modifies more the thermodynamics that regulates the stability of possible structural isomers of the Ru−complex, rather than the kinetics of the **A** → **C** conversion.

The decomposition pathway discussed so far is the one that seems to be preferred according to our calculations. Nevertheless, we also tested other possibilities. Beside the alternative pathway in which a CO molecule first displaces the $PMe_3$ ligand, path **b** in Figure 1, we investigated the possibility that CO binding to the (pre)catalyst **1a**, leading to **2a**, could promote $PMe_3$ dissociation from **2a**. Surprisingly, as we removed the $PMe_3$ ligand from **2a** the geometry optimization collapsed into the metallacycle structure of Figure 4. This structure is 23.0 kcal/mol above **2a**, which rules out this possibility. This result evidences once more the remarkable activating role of a $\pi$-acid ligand trans to the Ru−ylidene bond.

Finally, we explored the energetics of the Buchner ring expansion step after cyclopropanation of the aromatic ring. To have more details on this reaction we investigated the four systems showed in Chart 3. Comparison between systems **15a-18a** and systems **15b-18b** allows to understand the effect of the ylidene group and of the methyl groups of the mesityl ligand on the energetics of the Buchner ring expansion step.

The energetics of this step is shown in Table 2. The clean result is that in all the cases a rather low energy barrier is found. Further, the ring expansion step in **17a** → **17b** can be directly compared with the ring expansion step **5a** → **6a** shown in Figure 1. Cleary, this step is even more facile in the Ru-complex **5a**, with a barrier of only 0.8 kcal/mol and an energy gain of 8.5 kcal/mol, versus a barrier of 2.7 kcal/mol and an energetic gain of 4.3 kcal/mol for the **17a** to **17b** conversion. In the case of a Ru−benzylidene bond, the ring expansion step would correspond to **18a** → **18b**. Interestingly, this system presents the highest barrier, 6.7 kcal/mol, and the ring expansion product is practically isoenergetic with the starting cyclopropane species.

***Table 2.*** Energetics, in kcal/mol, of the Buchner Ring Expansion Step[a]

| system | $\Delta G^{\ddagger}_{Buch}$ | $\Delta G_{Buch}$ |
|---|---|---|
| **15** | 4.9 | −4.0 |
| **16** | 2.2 | −5.4 |
| **17** | 2.7 | −4.3 |
| **18** | 6.7 | −0.1 |

[a] $\Delta G^{\ddagger}_{Buch}$ is the activation energy of the ring expansion, while $\Delta G_{Buch}$ is the energy difference between the heptatriene product and the cyclopropyl species of Chart 3.

## Conclusions

Inspired by the experimental results of Diver and co-workers, who explored the reactivity induced by coordination of CO to the Ru atom of typical NHC-based olefin metathesis catalysts, we clarified the mechanistic details of this transformation. Our calculations clearly indicate that CO binding to the Ru center promotes a cascade of reactions with very low energy barriers that lead to the final crystallographically characterized product. Analysis of the relevant MOs, supported by dynamics simulations, illuminates the key role of the $\pi$-acid CO coordinated trans to the Ru−methylidene bond. Basically, it attracts electron density from the Ru, which results in reduced Ru backdonation to the $\pi$ MO on the methylidene group. The reduced electron density on the $\pi$ MO of the methylidene group allows for a favorable interaction with the $\pi$-aromatic system of the proximal mesityl group, which leads to metallacycle formation first and subsequently in the formation of a tensioned cyclopropane structure that finally evolves to the experimental product via a Buchner type ring expansion.

Furthermore, we expanded the scope of this work to investigate to which extent a large set of $\pi$-acid groups that can be normally present during olefin metathesis could promote this deactivating reaction. Our results clearly indicate that several $\pi$-acid groups can promote this deactivation route. However, this group must be able to approach the Ru center in the sterically protected coordination position trans to the Ru−methylidene bond. Finally, our comparative analysis indicated that the role of the $\pi$-acid is not kinetic in nature (i.e., in lowering the energy barrier for attack of the ylidene group to the proximal mesityl ring) but rather thermodynamic (i.e., in making the metallacycle species a stable intermediate that can further evolve).

**Acknowledgment.** We thank Dr. R. Rousseau, Pacific Northwest National Laboratory, for providing us the Ru pseudopotential and basis set for the CP2K simulations. This project has been supported by the European Community (FP7 Project CP-FP 211468-2 EUMET). We thank ENEA (www.enea.it) and the HPC team for support as for using the ENEA-GRID and the HPC facilities CRESCO (www.cresco.enea.it) Portici (Naples), Italy and BSC (Altamira Project QCM-2009-1-0006) for access to remarkable computational resources. A.P. thanks the Generalitat de Catalunya for a Beatriu de Pinós postdoctoral contract.

**Supporting Information Available:** Complete author list for ref 15, Cartesian coordinates, energy and a 3D sketch of the structures, and an MPG movie of the CP2K simulation. This material is available free of charge via the Internet at http://pubs.acs.org.

JA902552M